Original Article

Comparative Histological Study on the Possible Effect of Adipose-Derived Mesenchymal Stem Cells versus Platelet Rich Plasma in Adriamycin-Induced Chronic Kidney Disease in Adult Male Albino Rat

Hala Hassan Mohamed, Nagwa Abdel Wahab Ahmed, Nariman Amin Hussein and Manal Ali Abdel Mohsen

Department of Histology, Faculty of Medicine, Cairo University, Cairo, Egypt

ABSTRACT

Introduction: Chronic kidney disease (CKD) is a worldwide health problem with rising morbidity & mortality. So, this model was performed to compare the possible effect of adipose tissue-derived stem cells against platelet-rich plasma on CKD induced by Adriamycin in adult male albino rats.

Materials and Methods: 46 adult male albino rats were classified into a donor group (n= 2) and 4 experimental groups (n= 44): Group I (Control group), Group II: rats received once i.v injection of Adriamycin (ADR) 6mg/kg. This group was subdivided into two subgroups including IIa where rats were sacrificed after one week and subgroup IIb where rats were sacrificed after seven weeks. Group III: rats received ADR then after one week, injected once i.v. by Mesenchymal Stem Cells (MSCs) 2x106 and Group IV: rats received ADR then after one week, injected with Platelet-rich plasma (PRP) 1ml/kg via i.p twice a week for six successive weeks. Blood samples were withdrawn to measure blood urea nitrogen (BUN) and creatinine levels in serum. Specimens were stained by Haematoxylin and Eosin (H&E), Masson's trichrome, Periodic acid Schiff reaction (PAS) stains, and caspase 3& desmin immunohistochemical stains. A fluorescent microscopic study to detect the PKH-26 labeled Adipose tissue-derived mesenchymal stem cells was also done.

Results: The results revealed degenerative features of renal specimens in subgroup IIa with declined kidney functions. These changes were aggravated in subgroup IIb, manifested by marked deposition of collagen fibers, total loss in brush border of many tubules with severe positive immunoreactivity for caspase-3 & desmin within the renal corpuscle. These results were further confirmed by statistical and morphometric analysis.

Conclusions: MSCs and PRP could attenuate Adriamycin-induced CKD and restore normal renal structure and functions. PRP was more effective in reducing damage and promoting the healing of renal tissues.

Received: 03 March 2024, **Accepted:** 04 May 2024

Key Words: Adriamycin, BUN, CKD, MSCs, PRP.

Corresponding Author: Hala Hassan Mohamed, PhD, Department of Histology, Faculty of Medicine, Cairo University, Cairo, Egypt, **Tel.**: +2 011 4888 0674, **E-mail:** dr.hala88@kasralainy.edu.eg

ISSN: 1110-0559, Vol. 48, No. 2

INTRODUCTION

Chronic kidney disease (CKD) has become a global major health issue[1]. It is described as a gradual reduction in kidney function. CKD is caused by long-term damage to the renal tissues, which may develop into end stage of renal disease (ESRD)[2]. CKD is a condition that worsens over time, resulting in severe morbidity and mortality. Current treatment options cannot help with the regeneration and functional recovery of kidney injury[3].

Drug therapy, dialysis and kidney transplantation are the most common treatments for renal disorders. Dialysis and kidney transplantation have improved the life quality and increased the survival rate of patients with ESRD. However, both treatments are costly and have several complications. Moreover, these options are associated with drug therapy limitations, difficulty of dialysis and insufficient donors for kidney transplantation. Therefore, there is a need to develop affordable and efficient new therapies to delay or reverse the progression of CKD[4,5].

Adriamycin (ADR) is a broad-spectrum anti-neoplastic antibiotic, commonly used to treat several malignancies[6]. Nephropathy induced by adriamycin is a well-known animal model, which mirrors histological changes observed in human CKD through focal segmental glomerulosclerosis. It is characterized by podocyte injury, fibrosis, tubulointerstitial inflammation and glomerular sclerosis. Because of histological damage, renal impairment occurs[7,8].

Mesenchymal stem cells (MSCs) are progenitor cells that have self-renewal capacity and can differentiate into multiple lineages. MSCs can be isolated from a range of tissues including adipose tissue and bone marrow. MSCs have gradually been used to treat a variety of disorders, mostly through repairing diseased cells and rebuilding normal cells. MSCs have proangiogenic, anti-inflammatory, and immunomodulatory properties[9,10].

Platelet-rich plasma (PRP) is a tiny amount of plasma containing an increased concentration of platelets. One of

DOI: 10.21608/ejh.2024.272096.2026

the most promising technologies is using PRP in tissue regeneration[11]. The concentration of growth factors that PRP naturally contains is principally responsible for its effects like platelet-derived growth factor (PDGF), endothelial vascular growth factor (VEGF), and growth factor-like insulin (IGF)[12].

The purpose of the current study is to evaluate and compare the possible effect of mesenchymal stem cells, derived from the adipose tissue, versus platelet-rich plasma on Adriamycin-induced chronic kidney disease in a rat model. Histological, immunohistochemical, morphometric and biochemical methods were applied in this work.

MATERIALS AND METHODS

Chemicals

A. Doxorubicin hydrochloride/ Adriamycin (Adriadox): in the form of lyophilized powder 50mg (catalog number 1225703) that was dissolved in 25ml of saline. It was purchased from RMPL PHARMA LLP, Mumbai, India.

B. Adipose tissue-derived mesenchymal stem cells (ADMSCs): PKH-26 labeled mesenchymal stem cells that were prepared at the unit of tissue culture in the Histology Department, Faculty of Medicine, Cairo University. They were prepared from minced rat perirenal tissue, added collagenase type 1, and centrifuged to obtain a high-density cell pellet. The pellet was resuspended in Dulbecco's Modified Eagle Medium (DMEM), Fetal Bovine Serum, and Penicillin-Streptomycin and cultured. Then they were labeled with Paul Karl Horan 26 (PKH-26) (catalog number MINI26)

C. Platelet Rich Plasma (PRP): PRP was obtained from the unit of tissue culture, Biochemistry Department at the Faculty of Medicine, Cairo University. Venous blood from rats was collected, centrifuged, and plasma collected. The top layer was removed, leaving 5 mL of plasma as PRP, stored at -20°C, and thawed.

Experimental animals

This study involved 46 adult male albino rats, aged around twelve weeks old, weighing 180 grams on average. The animals were purchased and bred in the Animal House. Animals were placed in hygienic cages, kept in clean properly ventilated rooms, and allowed free access to diet and water. The study was conducted following the ethical policies and procedures of the Animal Committee of ethics of Kasr Al-Ainy, Faculty of Medicine, Cairo University (CU-IACUC) (approval number CU/III/F/23/22).

The study design

Rats were divided into four groups in addition to a donor group:

Donor Group: It included 2 rats that were used for the preparation of ADMSCs.

Group I (Control group), 16 rats: Rats were subdivided into 4 subgroups, 4 rats each as follows:

- Subgroup IA: Included normal animals that did not receive any medication or underwent any surgical intervention. Rats were sacrificed after seven weeks.
- Subgroup IB: Each rat received one i.v injection of about 0.5 ml saline, through the tail vein. They were sacrificed with subgroup IIb.
- Subgroup IC: Each rat received as Subgroup IB. Then one week later, rats also received an i.v injection of about 0.5 ml of phosphate-buffered saline (PBS) once and were sacrificed with group III.
- Subgroup ID: Each rat received as Subgroup IB. Then one week later, rats received intraperitoneal injections of an average of 0.2 ml saline twice a week. Rats were sacrificed with group IV.

Group II (Adriamycin group), 12 rats: Induction of CKD was induced by injection of Adriamycin (Adriadox, 50 mg powder was dissolved in 25ml of saline, RMPL PHARMA LLP, Mumbai, India). Each rat received one injection of Adriamycin (ADR) in a dose of 6mg/ kg (average 1.1mg/each rat) dissolved in 0.5 ml saline, via tail vein[13]. This group was subdivided according to time of sacrification into:

- Subgroup IIa (Adriamycin, 1 week): It included 4 rats that were sacrificed after one week to confirm the establishment of chronic kidney damage.
- Subgroup IIb (Adriamycin, 7 weeks): It included 8 rats that were sacrificed after seven weeks[14].

Group III (MSCs- treated group), 8 rats: Each rat received ADR with the exact route & dose as in group II. One week later, each rat received a single i.v injection of 2x106 MSCs in 0.5 ml of PBS, in the tail vein and then sacrificed after seven weeks[15,16].

Group IV (PRP treated group), 8 rats: Each rat was given ADR exactly as in group II. One week later, rats received a dose of 1ml/kg PRP (average 0.2 ml/each rat) via intraperitoneal injection (i.p) twice a week till the experiment ended (seven weeks after ADR injection)[17].

Animals were sacrificed by i.p. injection of thiopental sodium 500 [Egyptian Int- Pharmaceutical Industries CO-(EIPCO)] in a dose of 50 mg/kg[18].

Preparation of adipose tissue-derived mesenchymal stem cells (ADMSCs)

According to the method used by Kelp *et al*., (2017) & Hendawy *et al*., (2021)[19,20], preparation of Paul Karl Horan 26 (PKH26)-labeled ADMSCs was performed at the unit of tissue culture, Histology Department.

Preparation of platelet-rich plasma (PRP)

PRP was purchased from the Biochemistry Department. The used protocol for the preparation of PRP was like that used previously by Karina *et al*., 2019[21].

Serological and Biochemical studies

Just before sacrification, samples from blood were collected from the rats' tail veins for the detection of BUN and creatinine levels in serum. These parameters were used for the assessment of renal damage and functional recovery.

The left kidneys were homogenized for detection of tissue malondialdehyde (MDA) as a marker of oxidative stress that was measured by Elisa kits. It was extracted by the dispersive liquid-liquid microextraction (DLLME) method and was measured by gas chromatography-mass spectroscopy (GC/MS). MDA is a harmful product of lipid peroxidation[22]. All the previous studies were done in the Biochemistry Department.

Histological study

The right kidney sections were fixed in formol saline at 10% concentration for paraffin block preparation. Paraffin sections (5-7μm) were exposed to the following:

i. Hematoxylin and Eosin stain[23]: to detect histological changes of kidney structure.

ii. Masson's trichrome stain[23]: to demonstrate the deposition of collagen fiber.

iii. Periodic Acid Schiff Reaction (PAS) staining[24]: to detect the state of brush borders and basal laminae of renal tubular cells.

iv. Immunohistochemical staining using the following primary antibodies[24]:

   1. Anti caspase-3 antibody (Rabbit polyclonal antibody, Thermo Scientific Laboratories (USA), cat. number RB-1197-R7): marker to demonstrate apoptosis. The positive reaction appeared as brown deposits in the cytoplasm. Positive tissue control was a specimen of human tonsils according to the data provided by the antibody manufacturer. The negative control section was one of the renal tissue specimens that underwent the same processing except for adding the primary antibody.

   2. Anti desmin antibody (Mouse monoclonal antibody [DE-U-10], Abcam plc, England, catalog number ab6322): marker used to assess the affection of podocytes. The cytoplasm of the positive response was colored brown. Positive tissue control was a specimen of rat colon, human skeletal muscle, and mouse cardiac muscle tissue according to the data provided by the antibody manufacturer. The negative control section was one of the renal tissue specimens by omitting the step of adding the primary antibody.

Sections for immunohistochemical staining exposed to antigen retrieval by boiling in citrate buffer at pH 6.0 for about 10 min. Then incubation with the primary antibody for an hour was done. SP Histostain kit system (LAB-SA system, San Francisco, USA) was used. Mayer's hematoxylin was used for counterstaining.

V. Detection of PKH26 labeled ADMCS in unstained sections by fluorescent microscope (Japan, 7M03285). Positive sections appeared as red fluorescent color in the glomeruli & tubules of the cortical kidney.

Positive tissue control was a specimen of the developing cortex showing young migrating neuron according to the datasheet provided by the antibody manufacturer. The negative control section was one of the renal tissue specimens where no homing of the labeled ADMCS had been occured, , so no red fluorescent color in kidney cells was detected in negative control sections.

Morphometric Studies

Data was achieved using the "Leica Qwin 500C" image analyzer system (Leica Imaging System Ltd, Cambridge, UK). Randomly chosen ten non-overlapping fields were used for each measurement. The number of the affected renal glomeruli was counted in H and E-stained specimens per low power field (x100 magnification measuring frame 116964.91 μm^2). The mean area percent of collagen deposition per low power field (x200), PAS-positive material per high power field (x400 inside a standard measuring frame of area 7286.67μm^2), caspase-3, and desmin-positive immunoreactivity per high power field (x400 inside a standard measuring frame of area 7286.67μm^2) were also measured.

Statistical Studies

The measurements obtained were examined using Statistical Package for Social Science (SPSS) version 16 (Chicago- USA). Then comparisons between different groups were made by one-way analysis of variance (ANOVA) and then post-hoc Tukey test. Findings were presented as mean ± standard deviation (SD). The differences were deemed statistically significant when the probability (p) value was less than 0.05[25].

RESULTS

Biochemical Results (Table 1, Histograms 1-3)

Regarding BUN, also creatinine levels in serum, with tissue malondialdehyde (MDA), the mean values of their levels for both subgroup IIa (Adriamycin, 1 week) and subgroup IIb (Adriamycin, 7 weeks) exhibited a significant rise compared to group I (control). Also, values of these measurements in subgroup IIb showed a significant rise compared to subgroup IIa. Moreover, group III (MSCs-treated group) together with group IV (PRP-treated group) exhibited a significant decline compared to subgroup IIb. In addition, group IV showed a significant decline as regards group III.

Immunofluorescent Results

Specimens of renal cortex of group III (MSCs -treated group) expressed homing of MSCs labeled with PKH26 in the glomeruli & tubules of the cortical kidney (Figure 1).

Hematoxylin and Eosin Results

Examination of renal sections in all control subgroups showed the normal histological appearance of the cortex comprised of Malpighian renal corpuscles (each is composed of a capsular space-enclosed glomerulus). PCTs exhibited narrow lumina bordered by cuboidal cells that were highly acidophilic in their cytoplasm and had vesicular rounded nuclei. DCTs displayed wide lumen and were bordered by cubical cells which have vesicular rounded nuclei and lighter acidophilic cytoplasm (Figure 2).

Sections of subgroup IIa showed distorted renal corpuscles and destruction of glomeruli with some shrunken glomeruli were also noticed. In addition, some renal corpuscles showed a wide capsular space. The epithelial lining cells of some tubules showed vacuolated cytoplasm and dark-stained pyknotic nuclei (Figures 3 A,B).

While specimens in subgroup IIb showed congested peritubular capillaries, distorted renal corpuscle with destruction of glomeruli, and widening of the capsular spaces. Most of the tubular lumina contains cellular debris in addition to the widening of the lumina some tubules and vacuolated cytoplasm of tubular epithelial lining cells. Shedding of tubular epithelial lining cells is detected (Figure 3C). Distorted renal tubules and peritubular congestion with focal areas of interstitial mononuclear infiltration were also demonstrated (Figure 3D).

Specimens from the renal cortex of group III showed almost preserved glomerular structure with normal capsular space. The PCTs showed narrow lumina while the DCTs showed wider lumina (Figure 4A). The preserved structure of glomerulus (G) with a slight widening of capsular space was noticed. Most PCTs showed normal architecture with pale vesicular nuclei of their cells (Figure 4B).

Specimens of group IV displayed an almost restored normal appearance of glomeruli & PCTs with almost normal capsular space. In addition, almost all cells of the tubules have pale vesicular nuclei (Figures 4 C,D).

The mean number of affected renal corpuscles (± SD) in subgroup IIa (67.19 ± 1.83 per low power field) and in subgroup IIb (88.07 ± 1.55 per low power field) revealed a significant rise as compared to group I (6.74 ± 0.98 per low power field). Also, subgroup IIb (88.07 ± 1.55 per low power field) exhibited a significant rise as compared to subgroup IIa (67.19 ± 1.83 per low power field). Group III (37.79 ± 1.71 per low power field) & group IV (19.27 ± 1.33 per low power field) showed a significant decline in comparison to subgroup IIb (88.07 ± 1.55 per low power field). Also, group IV (19.27 ± 1.33) displayed a significant decrease compared to group III (37.79 ± 1.71 per low power field) [Table 2, Histogram 4].

Masson's Trichrome Results

Specimens from the cortex in group I (control group) exhibited typical collagen distribution (Figure 5A). While sections of subgroup IIa (Adriamycin, 1 week) showed more distribution of collagen within capillaries of glomeruli and in between the kidney tubules (Figure 5B). Subgroup IIb (Adriamycin, 7 weeks) exhibited marked deposition of collagen fibers (Figure 5C).

Specimens of group III (MSCs-treated group) displayed moderate deposition of collagen fibers (Figure 5D). Also, sections of group IV (PRP-treated group) displayed fewer distribution of collagen within capillaries of glomeruli and in between the kidney tubules (Figure 5E).

PAS-Stained Sections Results

Sections in group I (control group) exhibited preserved brush border and distinct basal laminae of multiple cortical tubules (Figure 6A). But sections of subgroup IIa (Adriamycin, 1 week) showed partial and complete loss of several tubules' brush borders. With interrupted basal laminae of some tubules (Figure 6B). Sections of subgroup IIb (Adriamycin, 7 weeks) displayed partially in addition to total loss of brush border in a lot of cortical renal tubules with interrupted basal laminae of some of the PCTs & DCTs (Figure 6C).

Whereas sections of group III (MSCs-treated group) showed intact brush borders in many tubules with interruption of basal laminae of some PCTs & DCTs (Figure 6D). In addition, sections of renal tubules in group IV (PRP-treated group) showed preserved brush borders & intact basal laminae in most of the cortical renal tubules (Figure 6E).

Immunohistochemical Stains

Caspase-3 Stained Sections Results

Sections of group I showed minimal positive cytoplasmic reactivity to caspase-3 within the renal corpuscles and tubules (Figure 7A). Whilst specimens of subgroup IIa displayed moderate cytoplasmic positive immunoreactivity of caspase-3 within kidney corpuscle & tubules (Figure 7B).

Sections of subgroup IIb exhibited marked cytoplasmic positive immunoreactivity of caspase-3 within the kidney corpuscle & tubules (Figure 7C). Sections of group III showed mild cytoplasmic immunoreactivity of caspase-3 within kidney corpuscle & tubules (Figure 7D). Sections from renal cortex group IV showed minimal reaction to caspase-3 within the cytoplasm of renal corpuscle & tubules (Figure 7E).

Desmin-Stained Sections Results

Sections in group I showed a negative reaction to desmin within glomeruli (Figure 8A). While sections of

subgroup IIa displayed moderate cytoplasmic positive immunoreactivity within glomeruli (Figure 8B).

Specimens of subgroup IIb exhibited strong cytoplasmic positive immunoreactivity within glomeruli (Figure 8C). Specimens of group III showed mild cytoplasmic immunoreactivity within glomeruli (Figure 8D). Specimens of group IV revealed minimal cytoplasmic immunoreactivity within glomeruli (Figure 8E).

Morphometric Results (Table 2, Histograms 4-8)

Regarding the number of affected renal corpuscles, the area percentage of collagen fibers, caspase-3, and desmin positive immunoreaction, values of subgroup IIa and subgroup IIb their values revealed a significant rise as compared to group I. Also, subgroup IIb exhibited a significant rise as compared to subgroup IIa. Group III & group IV showed a significant decline in comparison to subgroup IIb. Also, group IV displayed a significant decrease compared to group III.

Concerning the area % of PAS- positive reaction, measurements in subgroups IIa & IIb displayed a significant decline as compared to group I. Subgroup IIb displayed a significant decline compared to subgroup IIa. Both groups III and IV displayed a significant rise in contrast with subgroup IIb. Group IV showed a significant increase as compared to Group III.

Immunofluorescent Results

PKH26 labeled ADMCS displayed intense red fluorescence by fluorescent microscope in the glomeruli & tubules of the cortical kidney demonstrating that they had been seeded in the renal tissue (Figure 1).

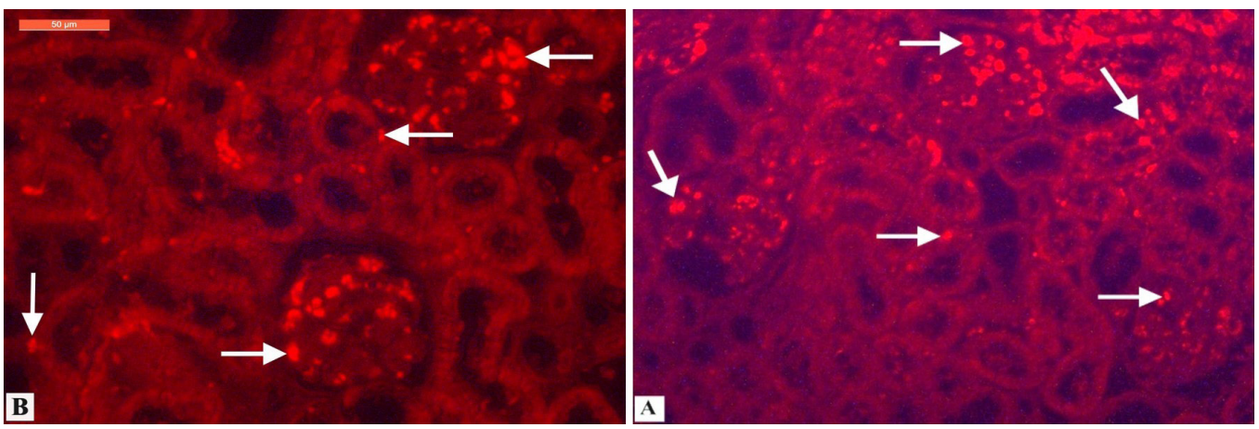

Fig. 1: photomicrographs of sections of group III (MSCs- treated group) display homing of the PKH 26- labeled MSCs in the glomeruli & cortical renal tubules (white arrows) (A: x200) (B: x400).

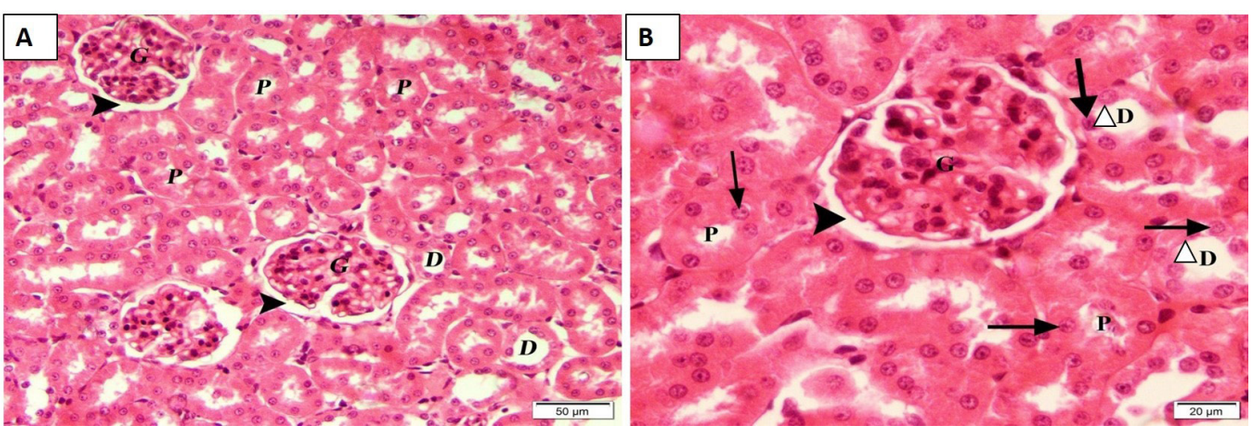

Fig. 2: [H& E]: A: photomicrograph from a section in group I (X 200) showing the normal histological appearance of the cortex comprised of Malpighian corpuscles composed of glomerulus (G) and capsular space (arrowheads) around. PCTs (P) with narrow lumina and DCTs (D) with wider lumina are also evident. B: Specimens of group I (X 400) showing PCTs bordered by high cells, cuboidal in shape with rounded vesicular nuclei & deeply acidophilic cytoplasm (arrows). While DCTs (D) have a wide lumen & are lined with cells having rounded vesicular nuclei, cubical and with lighter acidophilic cytoplasm (triangles).

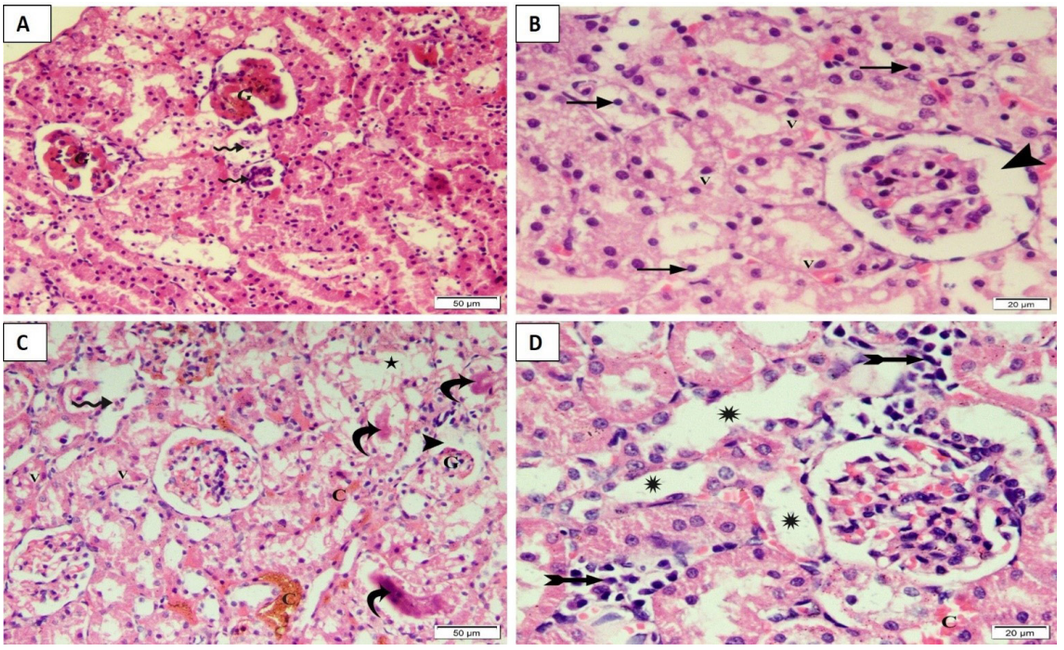

Fig. 3: [H& E]: A (x 200): a photomicrograph from a section of the renal cortex in subgroup IIa (Adriamycin, 1 week) displaying distorted renal corpuscles with destruction of glomeruli (G) with some shrunken glomeruli (spiral arrows). B (X 400): showing widening of the capsular space of Malpighian renal corpuscle (arrowhead). Vacuolated cytoplasm (V) & dark-stained nuclei (arrows) of the tubular epithelial lining cells. C (x 200): A photomicrograph of a section in subgroup IIb (Adriamycin, 7 weeks) showing congested peritubular capillary (C), distorted renal corpuscle with destruction of glomeruli (G), and widening of the capsular space (arrowhead). Most lumina have cellular debris (curved arrows). A widened tubular lumen (star) is also noted. Vacuolated cytoplasm (V) of tubular epithelial lining cells is also evident with the shedding of tubular epithelial lining cells (spiral arrow). D (x 400): Section of subgroup IIb showing distorted renal tubules (astrix), peritubular vascular congestion (C) with focal areas of interstitial mononuclear

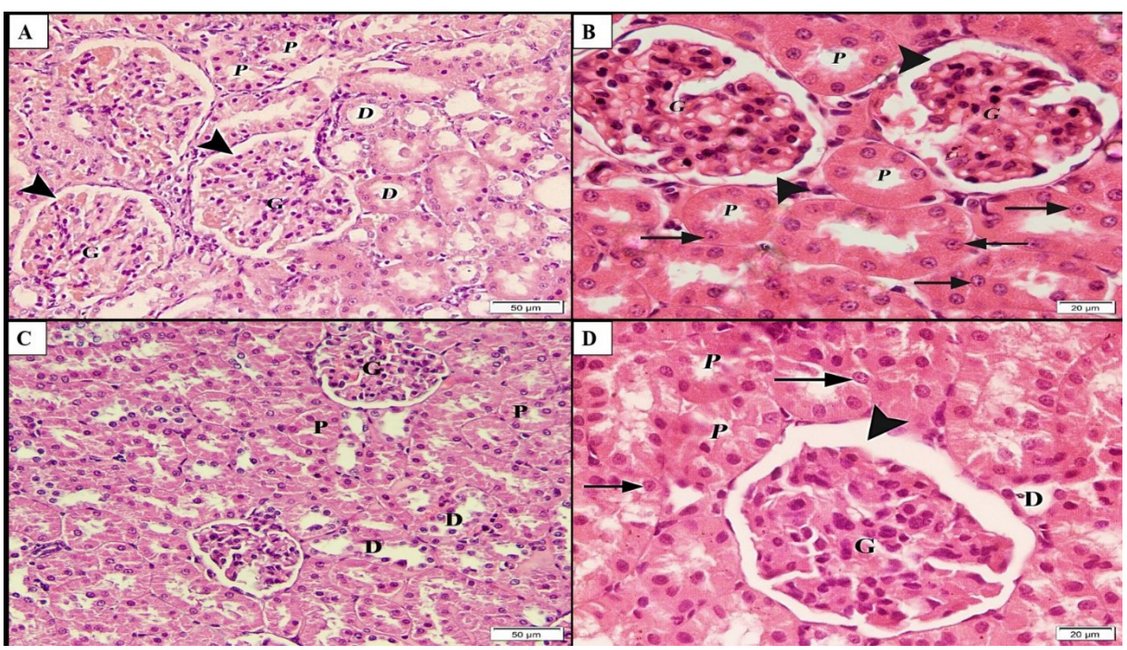

Fig. 4: [H& E]: A (x 200): Photomicrograph from section of group III (MSCs treated group) displaying an almost preserved glomerular (G) structure with some congestion with almost normal width of the capsular space (arrowheads). A lot of the PCTs (P) &DCTs (D) are almost apparently histologically normal. B (x 400): Section from the renal cortex in group III showing the preserved structure of glomerulus (G) with a slight widening of capsular space capsular space (arrowhead). Many tubular cells of the PCT (P) have pale vesicular nuclei (arrows). C (x 200): A section in the renal cortex of group IV (PRP-treated group exhibiting preserved normal structure of the glomeruli (G). With the apparently normal structure of most of the PCTs (P) and DCTs (D). D (x 400): A section in the renal cortex showing almost restored normal glomerular structure (G) with capsular space (arrowheads). PCTs (P) show preserved structure and nearly every tubule cell has a pale nucleus (arrows).

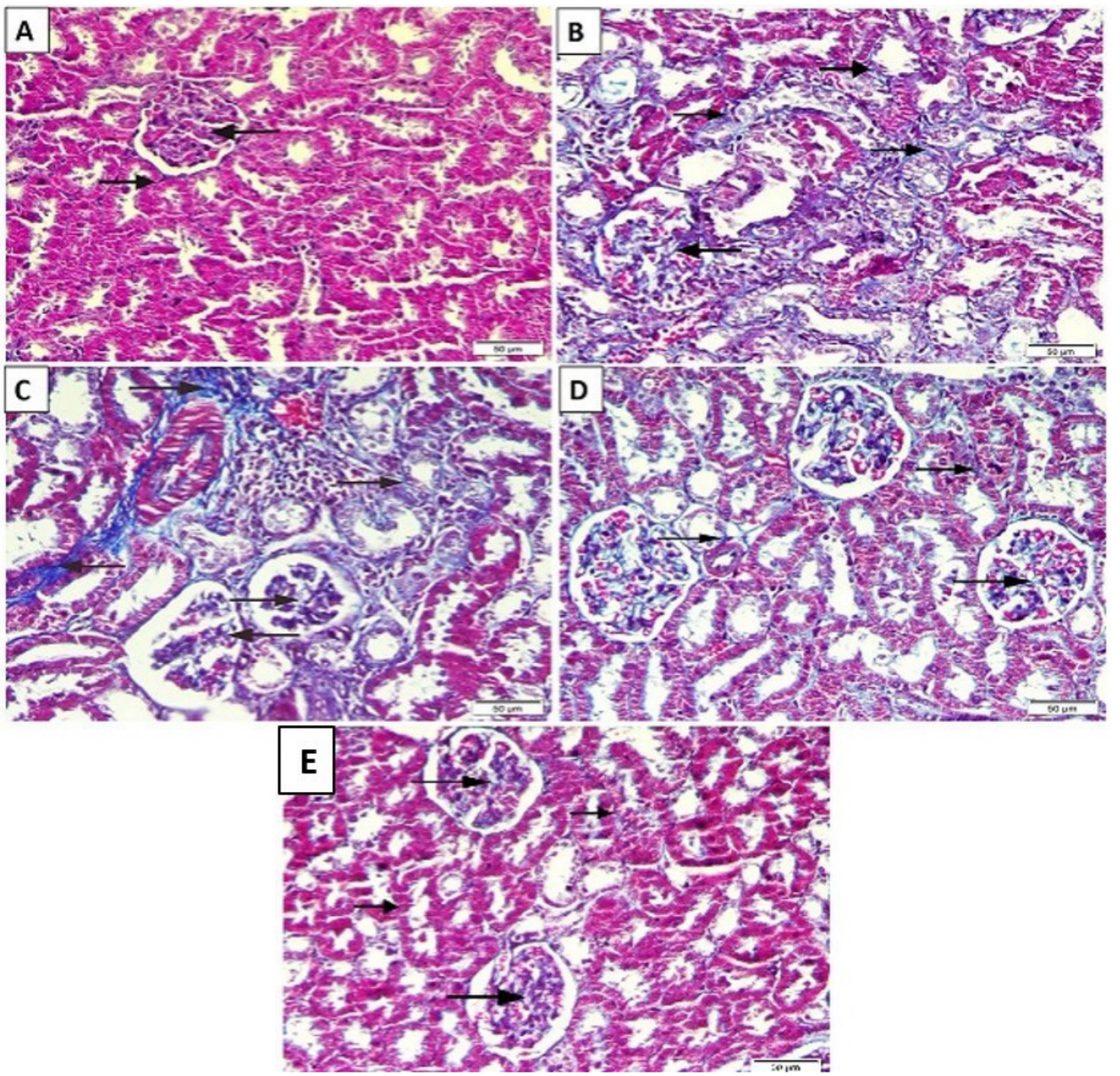

Fig. 5: (Masson trichrome x200): photomicrograph from a section in the renal cortex in group I (A): displaying the normal deposition of collagen fibers (arrows) within glomerular capillaries & among renal tubules. Subgroup IIa (B): showing more collagen distribution (arrows) in glomerular capillaries and among tubules. Subgroup IIb (C): exhibiting marked deposition of collagen fibers (arrows). Group III (D): shows moderate deposition of collagen fibers (arrows). Group IV (E): showing fewer distribution of collagen (arrows) within glomerular capillaries & between the tubules.

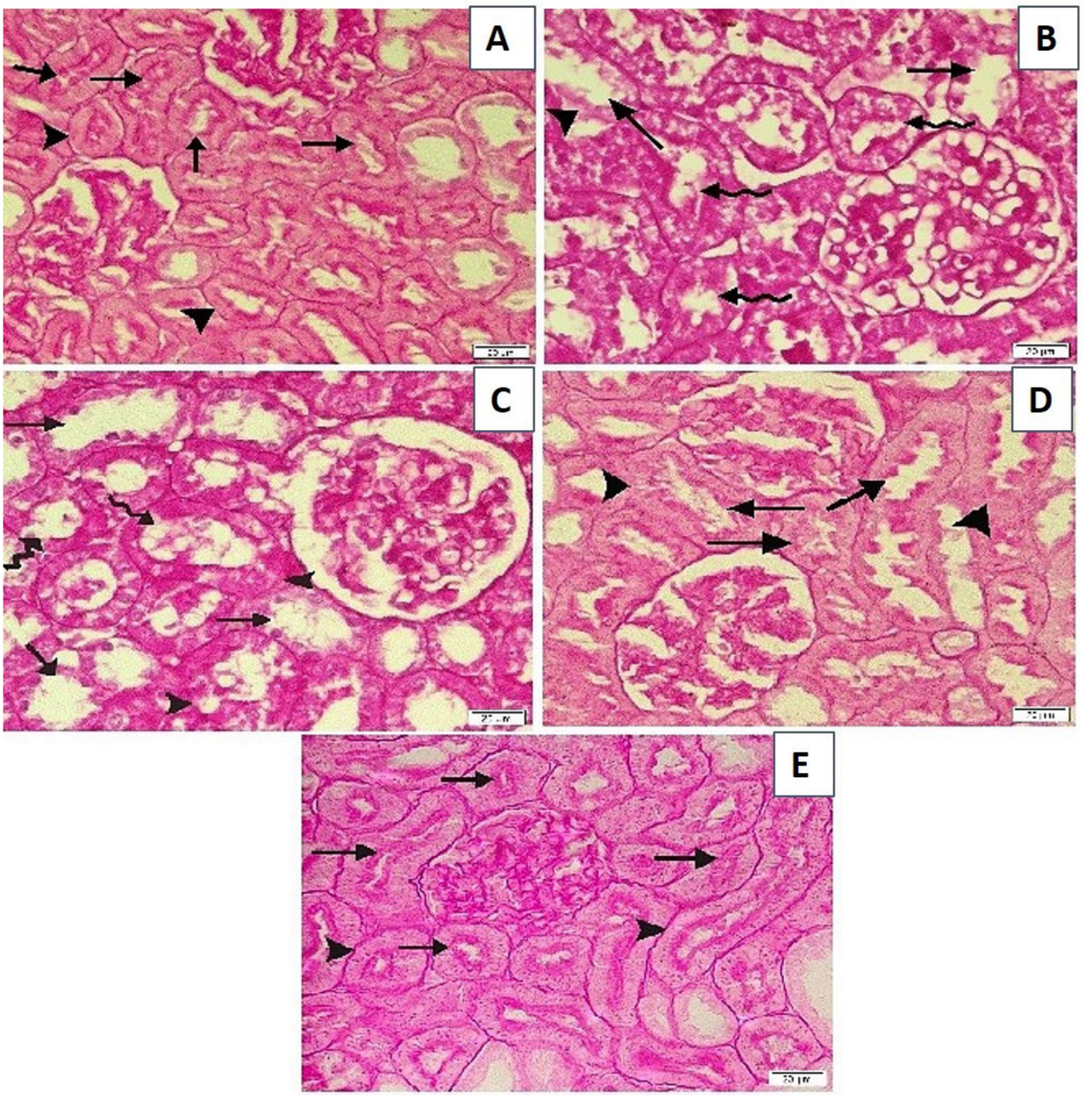

Fig. 6: (PAS x400): A section of group I (A): showing preserved brush border (arrows) and distinct basal laminae of multiple cortical tubules (arrowheads). Subgroup IIa (B): showing partial (spiral arrows) & complete disappearance of the brush border in many tubules (arrows). Interrupted tubular lamina (arrowhead) is also evident. Subgroup IIb (C): exhibiting partial (spiral arrows) and total (arrows) disappearance of the brush border from most tubules with interrupted basal lamina in some PCTs & DCTs (arrowheads). Group III (D): showing preserved brush border (arrows) in many tubules with interrupted laminae of some PCTs & DCTs (arrowheads). Group IV (E): showing preserved brush borders (arrows) & basal laminae of a lot of tubules (arrowheads).

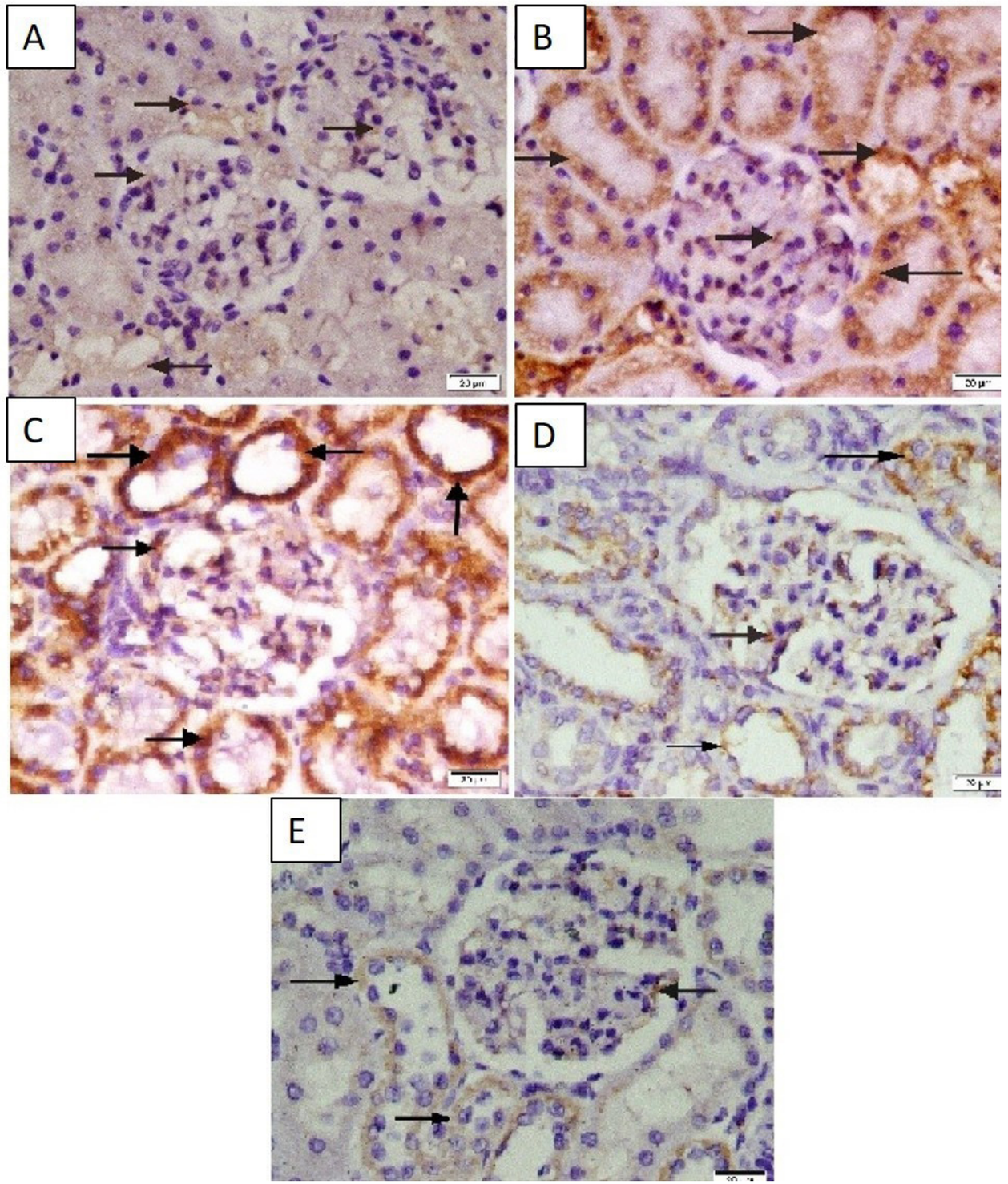

Fig. 7: (Caspase-3 immunostaining x400): photomicrograph of sections from renal cortex of group I (A): displaying minimal positive immunoreactivity in the cytoplasm (arrows) to caspase-3 within renal corpuscles together with renal tubular cells. Subgroup IIa (B): demonstrating moderate cytoplasmic positive immunoreactivity (arrows) within renal corpuscle and renal tubular cells. Subgroup IIb (C): exhibiting marked cytoplasmic positive immunoreactivity (arrows) to caspase-3 in renal corpuscles and tubular cells. Group III (D): showing mild cytoplasmic immunoreactivity (arrows) for caspase-3 within renal corpuscle and renal tubular cells. Group IV (E): showing minimal cytoplasmic immunoreactivity (arrows) in renal corpuscle and renal tubular cells.

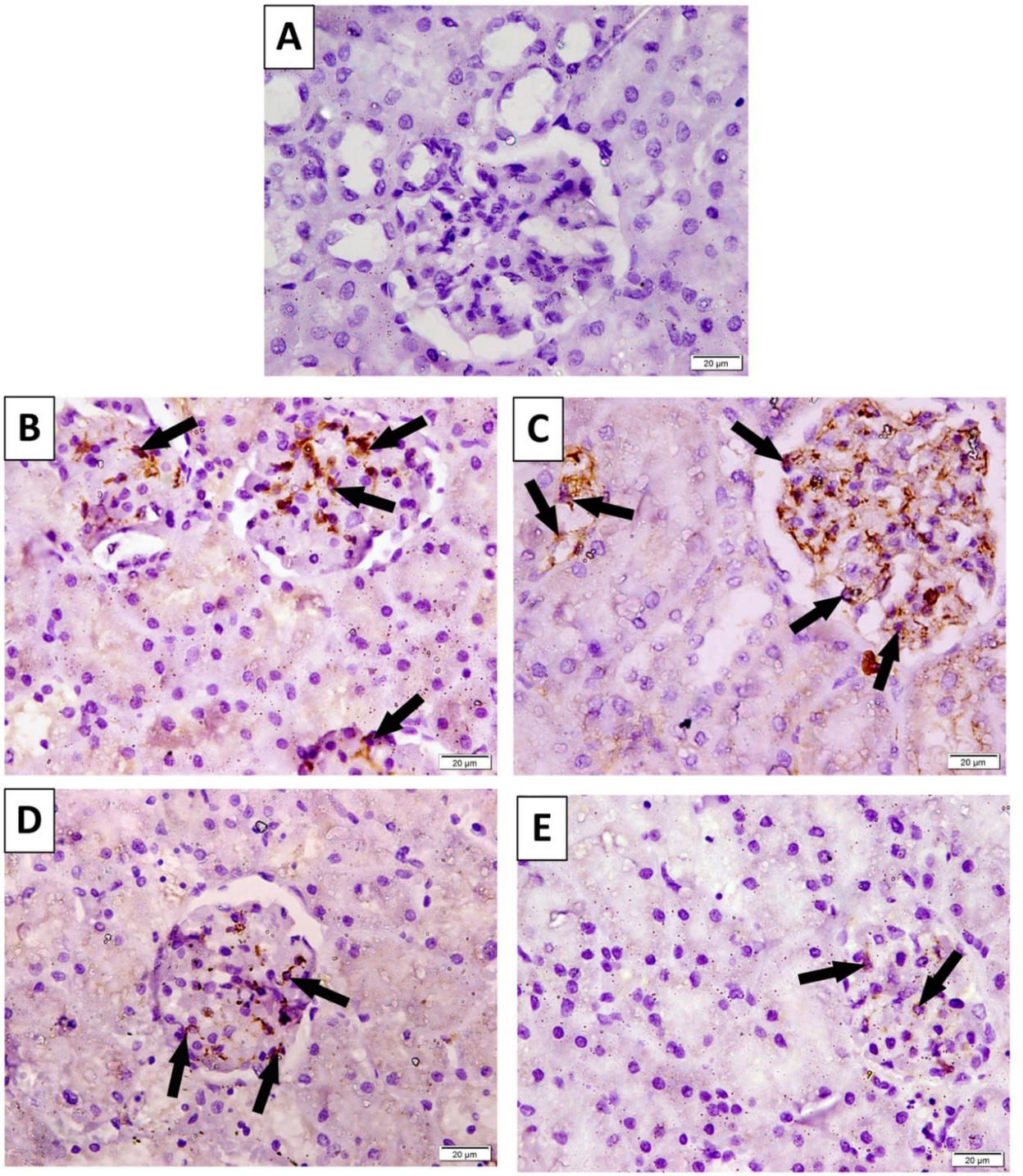

Fig. 8: (Desmin immunostaining x400): photomicrograph from sections in renal cortex in group I (A): displaying negative reaction for desmin within glomerulus. Subgroup IIa (B): demonstrating moderate cytoplasmic positive immunoreactivity (Thick arrows) within glomeruli. Subgroup IIb (C): exhibiting strong cytoplasmic positive immunoreactivity (Thick arrows) within glomeruli. Group III (D): showing mild cytoplasmic immunoreactivity (Thick arrows) within the glomerulus. Group IV (E): showing minimal cytoplasmic immunoreactivity (Thick arrows) within the glomerulus

Table 1: Values of serum BUN in (mg/ dL), levels of serum creatinine (mg/ dL) & tissue MDA (nanomolar/mg protein) (± SD) in the studied groups.

Groups	Mean serum blood urea nitrogen (mg/dl) ± SD	Mean serum creatinine (mg/dl) ± SD	Mean tissue MDA (nanomolar/mg protein) ± SD
Group I	23.95 ± 2.1	0.26 ± 0.07	35.9 ± 1.86
Subgroup IIa	63.3 ± 2*	1.62 ± 0.09*	90.01 ± 3.54*
Subgroup IIb	85.73 ± 1.42*^	2.32 ± 0.37*^	128.65 ± 1.31*^
Group III	40.77 ± 1.79#*	0.95 ± 0.11#*	70.39 ± 7.08#*
Group IV	32.75 ± 1.38#•*	0.6 ± 0.09#•*	55.66 ± 1.12#•*

* Significant rise compared to control (p<0.05).

^ Significant rise compared to subgroup IIa (p<0.05).

Significant decrease in relation to subgroup IIb (p<0.05).

• Significant decrease compared to group III (p<0.05).

Table 2: Mean number (± SD) in affected kidney corpuscles in low- power fields x 200, mean area % (± SD) of collagen in low- power fields x 200, caspase 3 using high- power fields x 400, desmin and PAS positive immunoreactivity using high- power fields x 400 inside a standard measuring frame of area (7286.67 µm^2).

Groups	Mean number of renal corpuscles (± SD)	Mean area percentage of collagen fibers (± SD)	Mean area percent of Caspase-3 positive immunoreactivity (± SD)	Mean area percent of Desmin positive immunoreactivity (± SD)	Mean area percentage of PAS-positive reaction (± SD)
Group I	6.74 ± 0.98	13.98 ± 2.55	3.02 ± 1.05	0.00	23.94 ± 1.86
Subgroup IIa	67.19 ± 1.83*	55.88 ± 4.47*	35.77 ± 2.33*	8.3±0.5*	8 ± 1.39*
Subgroup IIb	88.07 ± 1.55*^	74.54 ± 4.71*^	52.79 ± 5.41*^	22.3±1.1*^	3.06 ± 0.47*^
Group III	37.79 ± 1.71#*	37.36 ± 2.56#*	23.91 ± 1.63#*	3.2±0.8 #*	12.88 ± 0.81#*
Group IV	19.27 ± 1.33#•*	24.97 ± 2.22#•*	15.09 ± 1.49#•*	2.5±0.6#•*	16.94 ± 0.92#•*

* Significant rise compared to control (p<0.05).

^ Significant rise compared to subgroup IIa (p<0.05).

Significant decrease in relation to subgroup IIb (p<0.05).

• Significant decrease compared to group III (p<0.05).

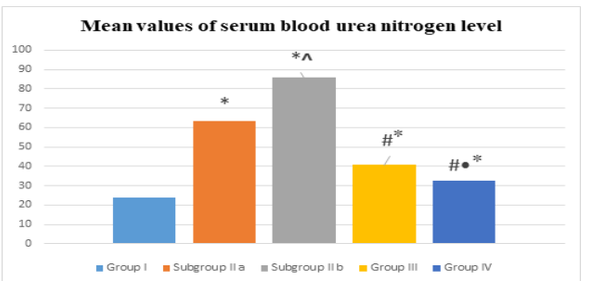

Histogram 1: Mean values of serum blood urea nitrogen in the studied groups: (*) Significant increase as compared to control group, (^) Significant increase as compared to subgroup IIa, (#) Significant decrease as compared to subgroup IIb, (•) Significant decrease as compared to group III (P < 0.05).

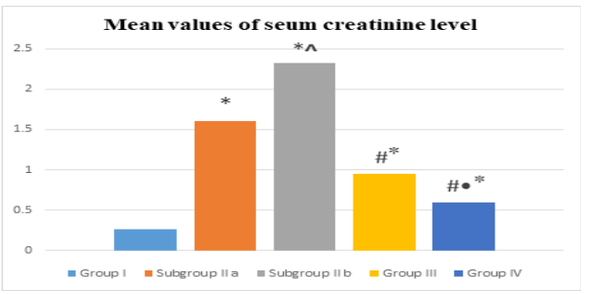

Histogram 2: Mean values of serum creatinine levels in the studied groups: (*) Significant increase as compared to control group, (^) Significant increase as compared to subgroup IIa, (#) Significant decrease as compared to subgroup IIb, (•) Significant decrease as compared to group III (P < 0.05).

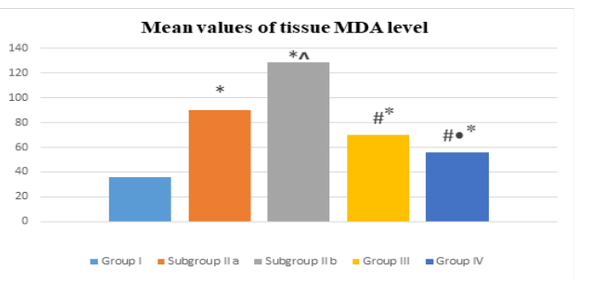

Histogram 3: Mean values of tissue MDA in the studied groups: (*) Significant increase as compared to control group, (^) Significant increase as compared to subgroup IIa, (#) Significant decrease as compared to subgroup IIb, (•) Significant decrease as compared to group III (P < 0.05)

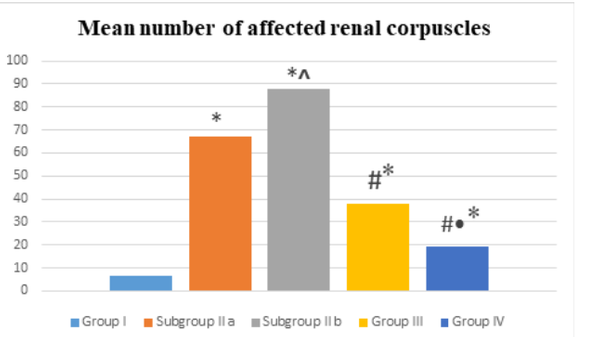

Histogarm 4: Mean number of affected renal corpuscles in the studied groups: (*) Significant increase as compared to control group, (^) Significant increase as compared to subgroup IIa, (#) Significant decrease as compared to subgroup IIb, (•) Significant decrease as compared to group III (P < 0.05).

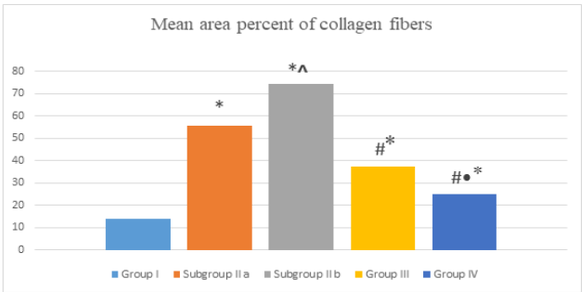

Histogarm 5: Mean area percent of collagen fibers in the studied groups: (*) Significant increase as compared to control group, (^) Significant increase as compared to subgroup IIa, (#) Significant decrease as compared to subgroup IIb, (•) Significant decrease as compared to group III ($P < 0.05$).

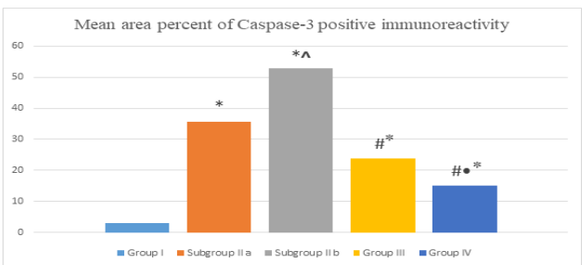

Histogarm 6: Mean area percent of Caspase-3 positive immunoreactivity in the studied groups: (*) Significant increase as compared to control group, (^) Significant increase as compared to subgroup IIa, (#) Significant decrease as compared to subgroup IIb, (•) Significant decrease as compared to group III ($P < 0.05$).

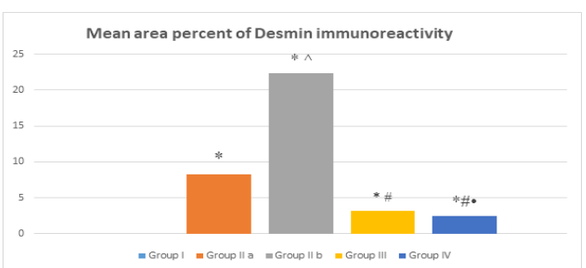

Histogarm 7: Mean area percent of Desmin positive immunoreactivity in the studied groups: (*) Significant increase as compared to control group, (^) Significant increase as compared to subgroup IIa, (#) Significant decrease as compared to subgroup IIb, (•) Significant decrease as compared to group III ($P < 0.05$).

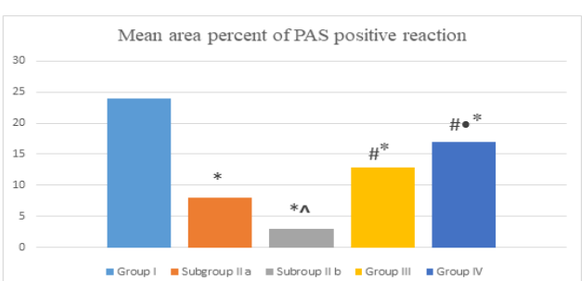

Histogarm 8: Mean area percent of PAS positive reaction in the studied groups: (*) Significant decrease as compared to control group, (^) Significant decrease as compared to subgroup IIa, (#) Significant increase as compared to subgroups IIb, (•) Significant increase as compared to group III ($P < 0.05$).

DISCUSSION

Chronic kidney disease (CKD) is known as a progressive disease which diminishes kidney function and causes kidney damage[26]. This study aimed at comparing the possible impact of adipose tissue stem cells versus platelet-rich plasma in CKD caused by Adriamycin in adult albino rats. Adriamycin (ADR) is preferred to induce chronic kidney disease as it can provide a model with histological changes like those found in human focal segmental glomerulosclerosis (FSGS)[27]. This disease can progress to glomerular sclerosis and fibrosis. These changes can appear as soon as 1-2 weeks after Adriamycin administration. The damage progressively increases and lasts more than six weeks after a single dose of Adriamycin[28,29].

In the present work, subgroup IIa displayed a significant rise in BUN in addition to serum levels of creatinine that were progressively elevated in subgroup IIb, suggesting deterioration of renal function. Similar results were previously reported by Lee and Harris, 2011 and Ding *et al*., 2013[28,13]. In addition, it was also documented that progressive elevation in renal function tests occurs after one week and up to sixty days after a single injection of ADR[14]. That can be due to the direct harmful impact of Adriamycin and tubular cell release of chemokines with subsequent oxidant damage[30].

Malondialdehyde (MDA) is recognized as a reliable marker to oxidative stress which is involved in tissue damage through DNA damage and lipid peroxidation together with modification of proteins. In this work, tissue MDA level was significantly elevated in subgroup IIa and more elevated in subgroup IIb. This was supported by a previous study that showed that Adriamycin-induced oxidative stress led to mitochondrial dysfunction, and damage of cellular components and membrane lipids. This causes lipid peroxidation and release of reactive aldehydes such as MDA[31].

In our study, sections stained with H&E of subgroup IIa revealed degenerative changes in the kidney architecture. These changes became aggravated in subgroup IIb which might indicate the progressive worsening of the condition. These changes appeared as the destruction of glomeruli with the widening of capsular space. Dilatation of renal tubules and the presence of debris inside their lumina were detected. Vacuolated cytoplasm, and dark pyknotic nuclei, in addition to the shedding of some cortical tubular epithelial cells were also evident. In addition, interstitial mononuclear cell infiltration together with congestion of peritubular capillaries was noticed. Damage was confirmed by morphometric measurements and analysis that revealed a significant progressive rise in the number of the affected glomeruli in both subgroups.

The current findings are similar to a previous study that reported distortion of glomeruli with dilated capsular space[32]. Also, marked renal tubular degeneration with exfoliation of their cells in addition to inflammatory cell infiltration and congestion were detected. Besides,

marked desquamation was noticed in the epithelial cells belonging to renal tubules[33]. Furthermore, condensation of chromatin of renal tubular cells may be considered as a sign of apoptosis induced after Adriamycin injection[34]. Previously mentioned findings clarified that Adriamycin-induced nephropathy is an ideal model of FSGS that results in renal impairment[35].

It was reported that a shrunken glomerular capillary tuft might explain the presence of widened capsular space[36]. The desquamation of epithelial cells lining the renal tubules could be attributed to severe oxidative stress of renal tubular cells[37]. In addition, the vacuolated cytoplasm of renal tubular cells is one of the important sequelae to cell damage, possibly due to increased cell membrane permeability[38]. Consequently, the cell accumulates water forming cytoplasmic vacuolation. FSGS can lead to progressive proteinuria which leads to tubulointerstitial injury that is manifested by severe inflammatory cell infiltration[14]. The presence of mononuclear cell infiltration was explained by the release of chemokines and cytokines as a result of the inflammatory response caused by injured renal epithelia[39].

The brush border and basal laminae of the renal convoluted tubules were evaluated by using a PAS stain[40]. In the current study, examination of PAS-stained specimens exhibited both partial & total disappearance of the brush border of the tubules with interrupted basal lamina in tubules of subgroup IIa and was exaggerated in subgroup IIb. It was previously reported that loss of tubular brush border occurs in adriamycin-treated animals[41]. The loss of tubular brush border was explained by Adriamycin-induced oxidative stress with subsequent formation of free radicals in the renal tissue[42]. The shedding of renal tubular cells by necrosis or apoptosis leads to tubular cells' detachment from the basement membrane leaving behind regions of the affected basement membrane[43]. The impaired integrity of basement membrane in chronic kidney disease results in proteinuria with injured tubules leading to interstitial inflammation and fibrosis together with collagen deposition[13].

Massons' trichrome stain is used for the detection of collagen deposition in renal tissue. This is considered an indicator of renal fibrosis in CKD[44]. In this work, renal sections revealed increased distribution of collagen between glomerular capillaries, and also between kidney tubules in subgroup IIa that became more severe in subgroup IIb. These results were further confirmed by morphometric & statistical analysis. Renal fibrosis was attributed to Adriamycin-induced inflammation and the elevated levels of transforming growth factor -β1 (TGF-β1) which is thought to be a crucial mediating factor in fibrosis development. It leads to increased secretion of extracellular matrix (ECM)[45]. Additionally, the process of renal fibrosis through the infiltration of inflammatory cells could be explained by proliferation and activation of fibroblasts, and tubular and microvascular degeneration. Chen *et al*., 2022 reported that the release of TGF-β1 is essential for triggering fibrosis and promoting its spread[46].

Caspase-3 is one of the Bcl-2 family which has a great role in the regulation of apoptosis and is used to detect apoptosis[47]. Increased positive cytoplasmic immunoreactivity for caspase-3 within the renal corpuscles and tubules was observed in subgroup IIa with a marked rise in subgroup IIb. Results were further established by morphometric and statistical studies. Increased expression of caspase-3 within renal corpuscles after one week of adriamycin administration was previously reported[48]. These findings were attributed to the action of Adriamycin which can induce apoptosis by increasing the apoptotic BAX gene's expression and inhibiting the expression of antiapoptotic Bcl-2 in an FSGS model[49].

In many chronic kidney disorders, the primary source of proteinuria and glomerular injury is podocyte destruction. In addition to serving as the mechanical and charge barriers, podocytes also control hydrostatic pressure and preserve the regular opening of glomerular capillary loops.

Podocyte damage and dysfunction result in proteinuria and glomerulosclerosis[50]. Desmin is an intermediate filament protein known to be an indicator of podocyte injury. In different glomerular diseases, expression was upregulated where podocytic injuries were found. The epithelial dedifferentiation of podocyte was accompanied by induction of markers like desmin. Elevation of transforming growth factor-β1 in the destroyed sections may lead to podocyte epithelial dedifferentiation and mesenchymal transition. However, desmin production in podocytes is thought to be a crucial indicator of the podocyte epithelial-to-mesenchymal transition as explained by Salem *et al*., 2017[51].

In this study, the treated group (group III) showed improvement regarding kidney functions as detected by significantly decreased levels of BUN, serum creatinine, and tissue MDA levels as compared to subgroup IIb. It was previously reported that MSCs could enhance renal function and lower levels of BUN & serum creatinine in a FSGS model[52]. Also, a significant reduction of MDA levels was reported after treatment of liver fibrosis with MSCs[53].

Regarding morphological alterations, H&E-stained sections of group III exhibited improvement in renal architecture. Most of the glomeruli appeared with preserved structure and normal capsular space. Also, most of the cortical kidney tubules showed apparently normal architecture. The morphometric analysis confirmed the findings observed in the glomeruli and revealed a statistically significant decline in the number of damaged glomeruli after MSC therapy. It was previously declared that MSCs can enhance renal tubular regeneration and restore renal function[54,30].

As regards PAS-stained sections, Group III showed preserved brush border in many tubules. This observation was previously reported by the restoration of renal tubular brush border after administration of MSCs[55]. Regarding Masson’s trichrome stain, results revealed an apparent

decrease in the collagen fibers within glomerular capillaries and between the kidney tubules, this was previously consistent with Almeida *et al*., 2022[56]. Concerning caspase-3 immunohistochemically stained sections of group III mild cytoplasmic immunoreactivity to caspase-3 within the corpuscles and tubules were observed. These results were previously documented Sarhan *et al*., 2014[57].

In the current study, MSCs migrated to the glomeruli and cortical renal tubules. That was confirmed by the homing of PKH26- labeled MSCs which showed red fluorescence colour when examined by fluorescent microscope. Chemokines are released in response to tissue injury. MSCs express receptors for various chemokines. Elevated levels of chemokines in the inflammatory sites direct MSCs to migrate to affected sites[58].

The previously mentioned findings elucidated the protective effects of MSC administration. These results were attributed to the release of different growth factors & cytokines that have anti-inflammatory in addition to anti-apoptotic, and regenerative functions[59]. Additionally, the MSCs' precise mechanisms for healing the damaged kidney may involve either trans-differentiation into tubular cells or paracrine mechanisms[43]. MSCs can differentiate into tubular epithelial cells and expand the proliferation of tubular cells. Furthermore, MSCs can produce enzymes that can detoxify ROS and manage oxidative damage[16]. Moreover, MSCs have an anti-fibrotic effect, that is achieved by increasing the expression of matrix metalloproteinase (MMP) and inhibiting TGF-β1 and macrophage infiltration[49]. Furthermore, the anti-apoptotic effect of MSCs was linked to their ability to inhibit the intrinsic apoptotic signaling pathway. MSCs reduce the expression of BAX and enhance the expression of Bcl-2. Thus, reducing the BAX/Bcl-2 ratio[60].

In our work, PRP- treated group (Group IV) showed obvious preservation of both the function and structure of renal tissues. As regards BUN, serum creatinine levels, and MDA levels, a significant reduction was detected in group IV as compared to subgroup IIb & group III. This suggests that PRP could protect against ROS and restore renal functions. Similar results were confirmed by Keshk and Zahran, 2019 & Hegab *et al*., 2019[17,30]. In this study, sections stained by H&E of group IV revealed almost restored normal glomerular and tubular structures. It was reported that apparent improvement in renal architecture occurs after treatment with PRP in a rat model of CKD[17].

PAS-stained specimens of group IV showed preserved brush border in lots of the tubules in addition to complete restoration of the tubular basal lamina. It was previously noticed that a strong positive PAS reaction in liver sections after treatment of hepatotoxicity with PRP[61].

Concerning Masson's trichrome stain, an almost normal deposition of collagen fibers among glomerular capillaries was restored consistent with a previous study that observed a significant reduction in the distribution of the collagen after administration of PRP in a rat model of fibrosis in the liver[62]. Similarly, it was reported that PRP can reduce fibrosis in gentamicin-treated rats[63]. Additionally, immunohistochemical stained renal sections of group IV revealed minimal cytoplasmic immunoreactivity for caspase-3 within renal corpuscle and tubules. This is consistent with a previous study that observed minimal caspase-3 immunoreactivity after treatment with PRP in a model of diabetic neuropathy in rats[64].

The results of the present work elucidated the nephroprotective effects of PRP. They increase the production of antioxidant enzymes to repair damage due to lipid peroxidation processes. It was also mentioned that PRP has antioxidant effects via reducing ROS generation[65]. The PRP releases a significant amount of growth factors including adenosine diphosphate (ADP), hepatocyte growth factor (HGF), and epidermal growth factor (EGF). It also produces insulin-like growth factor 1 (IGF-1) & adenosine triphosphate (ATP). Such growth factors help to regenerate renal tubular cells and restore renal function and kidney structure after injury[66]. Similarly, PRP houses various amounts of growth factors and cytokines, which can play an important role in the proliferation, vascularization, differentiation, and regeneration of cells together with their anti-fibrotic and anti-inflammatory characteristics[67].

Moreover, the anti-fibrotic role of PRP is attributed to its content of hepatocyte growth factor (HGF) that has anti-fibrotic activity in the kidney[63]. This function is achieved by opposing the action of TGF-β1 with subsequent inhibition of interstitial fibroblasts' activity. Additionally, PRP is postulated to have anti-apoptotic activity by reducing the expression of apoptotic genes[68].

CONCLUSION

Administration of MSCs and PRP enhanced the recovery of Adriamycin-induced kidney damage both structurally and functionally. However, the therapeutic effect of PRP in the treatment of Adriamycin-induced CKD was better than that of ADMSCs.

CONFLICT OF INTERESTS

There are no conflicts of interest.

REFERENCES

1. Uehara Y, Furusawa Y, Islam MS, Yamato O, Hatai H, Ichii O, Yabuki A (2022) Immunohistochemical Expression of TGF-β1 in Kidneys of Cats with Chronic Kidney Disease. Vet Sci 9(3): 114. doi: 10.3390/vetsci9030114.
2. Akchurin OM (2019) Chronic Kidney Disease and Dietary Measures to Improve Outcomes. Pediatr Clin North Am 66(1): 247-267. doi: 10.1016/j.pcl.2018.09.007.
3. Yun CW, Lee SH (2019) Potential and Therapeutic Efficacy of Cell-based Therapy Using Mesenchymal Stem Cells for Acute/chronic Kidney Disease. Int J Mol Sci 20(7): 1619. doi: 10.3390/ijms20071619.

4. Huang Y, Yang L (2021) Mesenchymal stem cells and extracellular vesicles in therapy against kidney diseases. Stem Cell Res Ther 12(1): 219. https://doi.org/10.1186/s13287-021-02289-7.

5. Liu Y, Guo W, Guo Y, Chen X, Liu W (2022) Bone marrow mesenchymal stem cell-derived exosomes improve renal fibrosis via regulating Smurf 2/Smad 7. Frontiers in Bioscience-Landmark 27(1): 17. doi: 10.31083/j.fbl2701017.

6. Mansouri E, Assarehzadegan MA, Nejad-Dehbashi F, Kooti W (2018) Effects of Pravastatin in Adriamycin-Induced Nephropathy in Rats. Iran J Pharm Res 17(4): 1413- 1419. PMID: 30568699; PMCID: PMC6269566.

7. Yang RC, Zhu XL, Wang J, Wan F, Zhang HQ, Lin Y, Tang XL, Zhu B (2018) Bone marrow mesenchymal stem cells attenuate the progression of focal segmental glomerulosclerosis in rat models. BMC Nephrol 19(1): 335. doi: 10.1186/s12882-018-1137-5.

8. Matsuyama T, Ohashi N, Aoki T, Ishigaki S, Isobe S, Sato T, Fujikura T, Kato A, Miyajima H, Yasuda H (2021) Circadian rhythm of the intrarenal renin-angiotensin system is caused by glomerular filtration of liver-derived angiotensinogen depending on glomerular capillary pressure in adriamycin nephropathy rats. Hypertens Res 44(6): 618-627. doi: 10.1038/s41440-021-00620-6.

9. Gao JG, Yu MS, Zhang MM, Gu XW, Ren Y, Zhou X, Chen D, Yan TL, Li YM, Jin X (2020): Adipose-derived mesenchymal stem cells alleviate TNBS-induced colitis in rats by influencing intestinal epithelial cell regeneration, Wnt signaling, and T cell immunity. World J of Gastroenterol 26(26): 3750-3766. doi: 10.3748/wjg.v26.i26.3750.

10. Dabrowska S, Andrzejewska A, Janowski M, Lukomska B (2021) Immunomodulatory and Regenerative Effects of Mesenchymal Stem Cells and Extracellular Vesicles: Therapeutic Outlook for Inflammatory and Degenerative Diseases. Front Immunol 11: 591065. doi: 10.3389/fimmu.2020.591065.

11. Sayed WM, Elzainy A (2021) Impact of platelet-rich plasma versus selenium in ameliorating induced toxicity in rat testis: histological, immunohistochemical, and molecular study. Cell Tissue Res 385(1): 223-238. doi: 10.1007/s00441-021-03439-2.

12. Geropoulos G, Psarras K, Giannis D, Martzivanou EC, Papaioannou M, Kakos CD, Pavlidis ET, Symeonidis N, Koliakos G, Pavlidis TE (2021) Platelet rich plasma effectiveness in bowel anastomoses: A systematic review. World J Gastrointest Surg 13(12): 1736- 1753. doi: 10.4240/wjgs.v13.i12.1736.

13. Ding ZH, Xu LM, Wang SZ, Kou JQ, Xu YL, Chen CX, Yu HP, Qin ZH, Xie Y. (2014) Ameliorating Adriamycin-Induced Chronic Kidney Disease in Rats by Orally Administrated Cardiotoxin from Naja naja atra Venom. Evid Based Complement Alternat Med 2014: 621756. doi: 10.1155/2014/621756.

14. Faleiros CM, Francescato HD, Papoti M, Chaves L, Silva CG, Costa RS, Coimbra TM (2017) Effects of previous physical training on adriamycin nephropathy and its relationship with endothelial lesions and angiogenesis in the renal cortex. Life Sci 169: 43- 51. doi: 10.1016/j.lfs.2016.11.014.

15. Bai YH, Jiang HY, Lian XY, Wang JS, Wang JP (2015) Influence of mesenchymal stem cells on expression of AQP1 and AQP2 in rats with nephropathy induced by adriamycin. Int J Clin Exp Med 8(9): 16083- 16088. PMID: 26629116; PMCID: PMC4659005.

16. Song IH, Jung KJ, Lee TJ, Kim JY, Sung EG, Bae YC, Park YH (2018) Mesenchymal stem cells attenuate adriamycin-induced nephropathy by diminishing oxidative stress and inflammation via downregulation of the NF-kB. Nephrology (Carlton) 23(5): 483- 492. doi: 10.1111/nep.13047.

17. Keshk WA, Zahran SM (2019) Mechanistic role of cAMP and hepatocyte growth factor signaling in thioacetamide-induced nephrotoxicity: Unraveling the role of platelet rich plasma. Biomed Pharmacother 109: 1078- 1084. doi: 10.1016/j.biopha.2018.10.121.

18. Rafsanjani FN, Adeli S, Ardakani ZV, Ardakani JV, Ghotbi p (2009) Effects of diabetes mellitus on gastric motility in rats. Pak j physiol 5(1). https://pjp.pps.org.pk/index.php/PJP/article/view/692

19. Kelp A, Abruzzese T, Wohrle S, Frajs V, Aicher W (2017) Labeling Mesenchymal Stromal Cells with PKH26 or VybrantDil Significantly Diminishes their Migration, but does not affect their Viability, Attachment, Proliferation and Differentiation Capacities. J Tissue Sci Eng 8(2): 1- 8. DOI:10.4172/2157-7552.1000199

20. Hendawy H, Kaneda M, Metwally E, Shimada K, Tanaka T, Tanaka R (2021) A Comparative Study of the Effect of Anatomical Site on Multiple Differentiation of Adipose-Derived Stem Cells in Rats. Cells 10(9): 2469- 2484. doi: 10.3390/cells10092469.

21. Karina, Samudra MF, Rosadi I, Afini I, Widyastuti T, Sobariah S, Remelia M, Puspitasari RL, Rosliana I, Tunggadewi TI (2019) Combination of the stromal vascular fraction and platelet-rich plasma accelerates the wound healing process: pre-clinical study in a Sprague-Dawley rat model. Stem Cell Investig 6: 18. doi: 10.21037/sci.2019.06.08.

22. Amin MM, Rafiei N, Poursafa P, Ebrahimpour K, Mozafarian N, Shoshtari Yeganeh B, Hashemi M, Kelishadi R (2018) Association of benzene exposure with insulin resistance, SOD, and MDA as markers of oxidative stress in children and adolescents. Environ Sci Pollut Res Int 25(34): 34046- 34052. doi: 10.1007/s11356-018-3354-7.

23. Kiernan JA (2015) Histological and histochemical methods, theory and practice. 5th ed., Scion Publishing Limited Press, 184- 206.
24. Suvarna K, Layton C, Bancroft J (2018) Bancroft's theory and practice of histological techniques E-book. Philadelphia: Elsevier health sciences, 180-185.
25. Altman N, Krzywinski M (2017) Points of significance: interpreting P values. Nature methods 14(3): 213-215. doi: 10.1038/nmeth.4210.
26. Yu A, Zhao J, Yadav SPS, Molitoris BA, Wagner MC, Mechref Y (2021) Changes in the Expression of Renal Brush Border Membrane N-Glycome in Model Rats with Chronic Kidney Diseases. Biomolecules 11(11): 1677. doi: 10.3390/biom11111677.
27. Bryant C, Cianciolo R, Govindarajan R, Agrawal S (2022) Adriamycin-Induced Nephropathy is Robust in N and Modest in J Substrain of C57BL/6. Front Cell Dev Biol 10: 924751. doi: 10.3389/fcell.2022.924751.
28. Lee VW. Harris DC (2011) Adriamycin nephropathy: a model of focal segmental glomerulosclerosis. Nephrology (Carlton) 16(1): 30- 38. doi: 10.1111/j.1440-1797.2010.01383.x.
29. Nogueira A, Pires MJ, Oliveira PA (2017) Pathophysiological Mechanisms of Renal Fibrosis: A Review of Animal Models and Therapeutic Strategies. In *vivo* 31(1): 1- 22. doi: 10.21873/in*vivo*.11019.
30. Hegab II, Abd-ellatif RN, Atef MM (2019) "Effect of platelet rich plasma on an experimental rat model of adriamycin induced chronic kidney disease. Med. J. Cairo Univ 87(3): 2207- 2217. doi: 10.21608/mjcu.2019.54382
31. Taskin E, Ozdogan K, Kunduz Kindap E, Dursun N (2014) The restoration of kidney mitochondria function by inhibition of angiotensin-II production in rats with acute adriamycin-induced nephrotoxicity. Ren Fail 36(4): 606- 612. doi: 10.3109/0886022X.2014.882737.
32. Afsar T, Razak S, Almajwal A, Al-Disi D (2020) Doxorubicin-induced alterations in kidney functioning, oxidative stress, DNA damage, and renal tissue morphology; Improvement by Acacia hydaspica tannin-rich ethyl acetate fraction. Saudi J Biol Sci 27(9): 2251- 2260. doi: 10.1016/j.sjbs.2020.07.011.
33. Wu Q, Li W, Zhao J, Sun W, Yang Q, Chen C, Xia P, Zhu J, Zhou Y, Huang G, Yong C, Zheng M, Zhou E, Gao K (2021) Apigenin ameliorates doxorubicin-induced renal injury via inhibition of oxidative stress and inflammation. Biomed Pharmacother 137:111308. doi: 10.1016/j.biopha.2021.111308.
34. Zhang Q, Wu G, Guo S, Liu Y, Liu Z (2020) Effects of tristetraprolin on doxorubicin (adriamycin)-induced experimental kidney injury through inhibiting IL-13/STAT6 signal pathway. Am J Transl Res 12(4): 1203-1221. PMID: 32355536; PMCID: PMC7191163.
35. Zhang X, Li T, Wang L, Li Y, Ruan T, Guo X, Wang Q, Meng X (2023) Relative comparison of chronic kidney disease-mineral and bone disorder rat models. Front Physiol 14:1083725. doi: 10.3389/fphys.2023.1083725.
36. El-Safti FE, Mohammed SA (2017) Light and electron microscopic studies of chronic renal failure using an adenine rat model. Menoufia Med J 30(1): 271-277. https://www.mmj.eg.net/article.asp?issn=1110-2098;year=2017;volume=30;issue=1;spage=271;epage=277;aulast=El%2DSafti
37. Zhou Y, Wu Q, Du Z, Huang M, Gao K, Ma X, Zhang H, Qiang S, Sun W. (2022) Verbena Attenuates Adriamycin-Induced Renal Tubular Injury via Inhibition of ROS-ERK1/2-NLRP3 Signal Pathway. Evid Based Complement Alternat Med 2022: 7760945. doi: 10.1155/2022/7760945.
38. Rahm MAM, Atty YHA, Rahman MMA (2017) Structural changes induced by gibberellic acid in the renal cortex of adult male albino rats. MOJ Anat Physiol 3(1): 21- 27. DOI: 10.15406/mojap.2017.03.00080
39. Gewin L, Zent R, Pozzi A (2017) Progression of chronic kidney disease: too much cellular talk causes damage. Kidney Int 91(3): 552- 560. doi: 10.1016/j.kint.2016.08.025.
40. Belaïd-Nouira Y, Bakhta H, Haouas Z, Flehi-Slim I, Ben Cheikh H (2013) Fenugreek seeds reduce aluminum toxicity associated with renal failure in rats. Nutr Res Pract 7(6): 466- 474. doi: 10.4162/nrp.2013.7.6.466.
41. Shao L, Fang Q, Ba C, Zhang Y, Shi C, Zhang Y, Wang J (2022) Identification of ferroptosis associated genes in chronic kidney disease. Exp Ther Med 25(1): 60. doi: 10.3892/etm.2022.11759.
42. Oguz F, Beytur A, Sarihan E, Oguz HK, Bentli R, Samdanci E, Kose E, Polat A, Duran ZR, Parlakpinar H, Ekinci N (2016) Protective effects of molsidomine against doxorubicin-induced renal damage in rats. Clin Invest Med 39(1):E7-14. doi: 10.25011/cim.v39i1.26325.
43. Sakr AI, Abd Elhai WM, Abo Zeid AA, Ali HE (2017) Transplanted Adipose Derived Mesenchymal Stem Cells Attenuate. The Acute Renal Injury Induced by Cisplatin in Rats. Egyptian Journal of Histology 40(2): 169- 183. DOI: 10.21608/EJH.2017.4075
44. Acikgoz Y, Can B, Bek K, Acikgoz A, Ozkaya O, Genç G, Sarikaya S (2014) The effect of simvastatin and erythropoietin on renal fibrosis in rats with unilateral ureteral obstruction. Ren Fail 36(2): 252- 257. doi: 10.3109/0886022X.2013.836936.
45. Wei MG, He WM, Lu X, Ni L, Yang YY, Chen L, Xiong PH, Sun W (2016) JiaWeiDangGui Decoction Ameliorates Proteinuria and Kidney Injury in Adriamycin-Induced Rat by Blockade of TGF-β/Smad Signaling. Evid Based Complement Alternat Med 2016: 5031890. doi: 10.1155/2016/5031890.

46. Chen R, Xu L, Zhang X, Sun G, Zeng W, Sun X. (2022) Protective effect and mechanism of Shenkang injection on adenine-induced chronic renal failure in rats. Acta Cir Bras 37(3): e370304. doi: 10.1590/acb370304.

47. Elblehi SS, El-Sayed YS, Soliman MM, Shukry M (2021) Date Palm Pollen Extract Avert Doxorubicin-Induced Cardiomyopathy Fibrosis and Associated Oxidative/Nitrosative Stress, Inflammatory Cascade, and Apoptosis-Targeting Bax/Bcl-2 and Caspase-3 Signaling Pathways. Animals (Basel) 11(3): 886. doi: 10.3390/ani11030886.

48. Zhu Y, Liu M, Xun W, Li K, Niu X (2022) P2X7R antagonist protects against renal injury in mice with adriamycin nephropathy. Exp Ther Med 23(2): 161. doi: 10.3892/etm.2021.11084.

49. Kim HS, Lee JS, Lee HK, Park EJ, Jeon HW, Kang YJ, Lee TY, Kim KS, Bae SC, Park JH, Han SB (2019) Mesenchymal Stem Cells Ameliorate Renal Inflammation in Adriamycin-induced Nephropathy. Immune Netw 19(5): e36. doi: 10.4110/in.2019.19.e36.

50. Chen X., Xiao J, Tao, D, Liang Y, Chen S, Shen L, Li S, Zheng Z, Zeng Y Luo C, Peng F, Long H (2024) Metadherin orchestrates PKA and PKM2 to activate β-catenin signaling in podocytes during proteinuric chronic kidney disease. Translational research: the journal of laboratory and clinical medicine 266: 68-83. doi: 10.1016/j.trsl.2023.11.006.

51. Salem M, Altayeb Z, El-Mahalaway A (2017) Histological and Immunohistochemical Study of Titanium Dioxide Nanoparticle Effect on the Rat Renal Cortex and the Possible Protective Role of Lycopene. Egyptian Journal of Histology 40(1), 80-93. DOI: 10.21608/EJH.2017.3700.

52. Yang JW, Dettmar AK, Kronbichler A, Gee HY, Saleem M, Kim SH, Shin JI (2018) Recent advances of animal model of focal segmental glomerulosclerosis. Clin Exp Nephrol 22(4): 752- 763. doi: 10.1007/s10157-018-1552-8.

53. Khalil MR, El-Demerdash RS, Elminshawy HH, Mehanna ET, Mesbah NM, Abo-Elmatty DM (2021) Therapeutic effect of bone marrow mesenchymal stem cells in a rat model of carbon tetrachloride induced liver fibrosis. Biomed J 44(5): 598-610. doi: 10.1016/j.bj.2020.04.011.

54. Özgermen BB, Bulut G, Pınarlı FA, Gültekin SS, Özen D, Yavuz O, Haydardedeoğlu AE (2022) Investigation of the effects of fetal rat kidney-derived mesenchymal stem cells implementation on doxorubicin-induced nephropathy in male Sprague–Dawley rats. Ankara Univ Vet Fak Derg 69: 201- 209. DOI: 10.33988/auvfd.822776

55. Ibrahim MA, Khalifa AM, Mohamed AA, Galhom RA, Korayem HE, Abd El-Fadeal NM, Abd-Eltawab Tammam A, Khalifa MM, Elserafy OS, Abdel-Karim RI (2022) Bone-Marrow-Derived Mesenchymal Stem Cells, Their Conditioned Media, and Olive Leaf Extract Protect against Cisplatin-Induced Toxicity by Alleviating Oxidative Stress, Inflammation, and Apoptosis in Rats. Toxics 10(9): 526. doi: 10.3390/toxics10090526.

56. Almeida A, Lira R, Oliveira M, Martins M, Azevedo Y, Silva KR, Carvalho S, Cortez E, Stumbo AC, Carvalho L, Thole A (2022) Bone marrow-derived mesenchymal stem cells transplantation ameliorates renal injury through anti-fibrotic and anti-inflammatory effects in chronic experimental renovascular disease. Biomed J 45(4): 629- 641. doi: 10.1016/j.bj.2021.07.009.

57. Sarhan M, El Serougy H, Hussein AM, El-Dosoky M, Sobh MA, Fouad SA, Sobh M, Elhusseini F (2014) Impact of bone-marrow-derived mesenchymal stem cells on adriamycin-induced chronic nephropathy. Can J Physiol Pharmacol 92(9): 733- 743. doi: 10.1139/cjpp-2013-0503.

58. Sadek EM, Afifi NM, Abd Elfattah LI, Abd-El Mohsen MA (2013) Histological study on effect of mesenchymal stem cell therapy on experimental renal injury induced by ischemia/reperfusion in male albino rat. Int J Stem Cells 6(1): 55- 66. doi: 10.15283/ijsc.2013.6.1.55.

59. Habib SA, Alalawy AI, Saad EA, El-Sadda RR (2022) Biochemical and histopathological evaluations of chronic renal failure rats treated with pluripotent human stem cells. Brazilian Journal of Pharmaceutical Sciences 58: e20089. doi.org/10.1590/s2175-97902022e20089

60. Wu HJ, Yiu WH, Wong DWL, Li RX, Chan LYY, Leung JCK, Zhang Y, Lian Q, Lai KN, Tse HF, Tang SCW (2017) Human induced pluripotent stem cell-derived mesenchymal stem cells prevent adriamycin nephropathy in mice. Oncotarget 8(61): 103640-103656. doi: 10.18632/oncotarget.21760.

61. El-sharouny SH, Rizk AA, Rashed AA, Sayed WM, Abd Elmoneam MDA (2019) Analysis of the therapeutic role of platelet-rich plasma against cisplatin-induced hepatotoxicity in rats: controversy between oxidative and apoptotic markers. Eur. J. Anat 23(3): 201- 213. https://www.eurjanat.com/v1/journal/paper.php?id=190138ar.

62. Abd Elzaher F, Moussa M, Raafat M, Emara M (2021) Histological Effect of Platelet Rich Plasma on CCL4 Induced Liver Fibrosis in Adult Albino Rat. Egyptian Journal of Histology 44(4): 932- 940. DOI: 10.21608/EJH.2020.51054.1390

63. Moghadam A, Khozani TT, Mafi A, Namavar MR, Dehghani F (2017) Effects of Platelet-Rich Plasma on Kidney Regeneration in Gentamicin-Induced Nephrotoxicity. J Korean Med Sci 32(1): 13- 21. doi: 10.3346/jkms.2017.32.1.13.

64. Ismail D, Farag E (2021) A Histological Study on Platelet Poor Plasma versus Platelet Rich Plasma in Amelioration of Induced Diabetic Neuropathy in Rats and the Potential Role of Telocyte-like Cells. Egyptian Journal of Histology 44(1): 8- 30. DOI: 10.21608/EJH.2020.27619.1274

65. Rizal DM, Puspitasari I, Yuliandari A (2020) Protective effect of PRP against testicular oxidative stress on D-galactose induced male rats. In AIP conference proceedings, AIP Publishing LLC 2260 (1): 040005. doi.org/10.1063/5.0015830

66. Salem NA, Hamza A, Alnahdi H, Ayaz N (2018) Biochemical and Molecular Mechanisms of Platelet-Rich Plasma in Ameliorating Liver Fibrosis Induced by Dimethylnitrosurea. Cell Physiol Biochem 47(6): 2331- 2339. doi: 10.1159/000491544.

67. Lin Y, Qi J, Sun Y (2021) Platelet-Rich Plasma as a Potential New Strategy in the Endometrium Treatment in Assisted Reproductive Technology. Front Endocrinol (Lausanne) 12: 707584. doi: 10.3389/fendo.2021.707584.

68. Salem N, Helmi N, Assaf N (2018) Renoprotective Effect of Platelet-Rich Plasma on Cisplatin-Induced Nephrotoxicity in Rats. Oxid Med Cell Longev 2018: 9658230. doi: 10.1155/2018/9658230.

الملخص العربى

دراسة هستولوچية مقارنة على التأثيرالمحتمل للخلايا الجذعية الوسيطة المشتقة من النسيج الدهنى مقابل البلازما الغنية بالصفائح الدموية علي اعتلال الكلية المزمن المحدث بالأدرياميسين في ذكرالجرذ الأبيض البالغ

هالة حسن محمد، نجوى عبد الوهاب أحمد، ناريمان أمين حسين، منال على عبد المحسن

قسم علم الأنسجة والخلايا، كلية الطب، جامعة القاهرة، مصر

الخلفية: يعتبرمرض الكلى المزمن مشكلة صحية في جميع أنحاء العالم مع ارتفاع معدلات الإصابة بالأمراض والوفيات. لذلك تم إجراء هذا النموذج لمقارنة التأثير المحتمل للخلايا الجذعية المشتقة من النسيج الدهني مقابل البلازما الغنية بالصفائح الدموية على اعتلال الكلى المزمن المحدث بواسطة الأدرياميسين في ذكور الفئران البيضاء البالغة.

الطرق والنتائج: أجريت هذه الدراسة على ٤٦ من ذكور الجرذان البيضاء البالغة، تم تقسيمهم إلى مجموعة مانحة وتشمل فأرين وأربع مجموعات تجريبية على النحو التالي: المجموعة الأولى (المجموعة الضابطة)، المجموعة الثانية (المجموعة المعالجة بعقار الأدرياميسين): حيث تلقى كل جرذ جرعة واحدة من عقار الأدرياميسين بمعدل ٦ مجم / كجم عن طريق الوريد الذيلى وقد تم تقسيم هذه المجموعة على حسب موعد التضحية إلى المجموعة الفرعية أ: حيث تمت التضحية بالجرذان بعد أسبوع للتأكد من حدوث تلف مزمن في الكلى و المجموعة الفرعية ب: حيث تمت التضحية بالجرذان بعد سبعة أسابيع. والمجموعة الثالثة (المجموعة المعالجة بالخلايا الجذعية الوسيطة): حيث تلقت الجرذان عقار الأدرياميسين بنفس جرعة و طريقة حقن المجموعة الثانية ثم بعد أسبوع واحد تلقى كل فأر جرعة ٢*١٠٦ من الخلايا الجذعية الوسيطة عن طريق الوريد الذيلى. والمجموعة الرابعة (المجموعة المعالجة بالبلازما الغنية بالصفائح الدموية): حيث تلقت الجرذان عقار اللأدرياميسين بنفس جرعة و طريقة حقن المجموعة الثانية. ثم بعد أسبوع واحد تلقى كل فأر جرعة ١ مل/كجم من البلازما الغنية بالصفائح الدموية عن طريق الحقن البريتونى مرتين في الأسبوع.

وتم سحب عينات الدم للكشف عن مستويات اليوريا نيتروجين والكرياتينين فى الدم وتم تجميع عينات الكلى وصباغتها بصبغة الهيماتوكسيلين والأيوسين وصبغة حمض شيف الأيودى وصبغة ماسون ثلاثية الالوان وكذلك الصبغة الهستوكيميائية المناعية ضد كاسباس ٣ وكذلك الديزمين. وقد أجريت دراسة مجهرية الفلورية للكشف عن الخلايا الجذعية الوسيطة المشتقة من النسيج الدهنى بصبغة PKH-٢٦.

النتائج: كشفت النتائج عن مظاهر تنكسية لعينات الكلى في المجموعة الفرعية IIa مع انخفاض وظائف الكلى. وتفاقمت هذه التغييرات في المجموعة الفرعية ،IIb والذى ظهر في ترسب ملحوظ لألياف الكولاجين، وفقدان كامل في حدود الفرشاة للعديد من الأنابيب مع نشاط مناعي إيجابي شديد ضد كاسباس ٣ وكذلك الديزمين داخل الجسم الكلوي. وقد تم تأكيد هذه النتائج بشكل أكبر من خلال التحليل الإحصائي والمورفومتري.

الإستنتاج: يمكن لكلا من الخلايا الجذعيه الوسيطة والبلازما الغنية بالصفائح الدموية أن يعالجا من مرض الكلى المزمن المحدث بالادرياميسين ويستعيدان البنية والوظائف الكلوية الطبيعية. ولكن وجد أن تأثير والبلازما الغنية بالصفائح الدموية أكثر فعالية في تقليل الضرر وتعزيز شفاء أنسجة الكلى.